



## Accelerated fatigue of dentin with exposure to lactic acid



Dominic Do<sup>a,1</sup>, Santiago Orrego<sup>a,1</sup>, Hessam Majd<sup>a</sup>, Heonjune Ryou<sup>a</sup>,  
Mustafa M. Mutluay<sup>a,c</sup>, Hockin H.K. Xu<sup>b</sup>, Dwayne D. Arola<sup>a,b,\*</sup>

<sup>a</sup> Department of Mechanical Engineering, University of Maryland Baltimore County, Baltimore, MD, USA

<sup>b</sup> Department of Endodontics, Prosthodontics, and Operative Dentistry, Dental School, University of Maryland, Baltimore, MD 21201, USA

<sup>c</sup> Adhesive Dentistry Research Group, Institute of Dentistry, University of Turku, Turku, Finland

### ARTICLE INFO

#### Article history:

Received 28 May 2013

Accepted 26 July 2013

Available online 13 August 2013

#### Keywords:

Cyclic crack growth

Demineralization

Dentin tubules

Fatigue

Fracture toughness

### ABSTRACT

Composite restorations accumulate more biofilm than other dental materials. This increases the likelihood for the hard tissues supporting a restoration (i.e. dentin and enamel) to be exposed to acidic conditions beyond that resulting from dietary variations. In this investigation the fatigue strength and fatigue crack growth resistance of human coronal dentin were characterized within a lactic acid solution (with pH = 5) and compared to that of controls evaluated in neutral conditions (pH = 7). A comparison of the fatigue life distributions showed that the lactic acid exposure resulted in a significant reduction in the fatigue strength ( $p \leq 0.001$ ), and nearly 30% reduction in the apparent endurance limit (from 44 MPa to 32 MPa). The reduction in pH also caused a significant decrease ( $p \leq 0.05$ ) in the threshold stress intensity range required for the initiation of cyclic crack growth, and significant increase in the incremental rate of crack extension. Exposure of tooth structure to lactic acid may cause demineralization, but it also increases the likelihood of restored tooth failures via fatigue, and after short time periods.

© 2013 Elsevier Ltd. All rights reserved.

## 1. Introduction

Resin composites have become the most common material for direct restoration of tooth cavities [1]. These materials have many desirable qualities, including better aesthetics, fewer health concerns to the patient and practitioner and they provide tooth reinforcement via adhesive bonding. Despite these advantages, the average clinical service life of resin composite restorations is lower than that of the materials they have replaced [2,3]. The primary modes of composite restoration failures are secondary caries, tooth fracture and degradation of the restorative margins. Approximately one half of all dental restorations fail within 10 years due to secondary caries and fracture [1,4,5].

Secondary caries result from the acid production of biofilms in the oral cavity [6,7]. Resin composites accumulate more biofilm/plaque than restorative materials of the past [8,9]. With prolonged attack, they may undergo a reduction in hardness and an increase in their surface roughness [10–12]. While the exact nature and

extent of degradation is resin dependent [11], the increase in surface roughness further encourages biofilm formation [12]. Changes to the surface topography of the composite may contribute to restoration failures via the increase in surface stress concentration and its affect on fatigue strength. Nevertheless, the acidic conditions also cause localized demineralization of the hard tissue foundation, which could foster degradation via cyclic loading.

For composite restorations to support lifelong oral health, the restorative materials and supporting dentin and enamel must resist damage over many years of function. Dentin occupies the majority of the tooth by both weight and volume. Microscopically, the most distinct feature of this tissue is the network of tubules (approx. 0.5–1.5  $\mu\text{m}$  in diameter) that radiate outward from the pulp cavity to the DEJ [7]. Regarded as the dentin tubules, each is embodied by a collagen free, hyper-mineralized cuff of peritubular dentin. The interstitial space between the peritubular cuffs, i.e. intertubular dentin, consists of a collagen fibril matrix reinforced by nanoscale crystals of apatite [13,14]. Owing to its complex composition and microstructure, dentin is often regarded as a hierarchical biological composite. Cyclic loads generated by mastication will result in cyclic stresses within the tooth, thereby causing fatigue of dentin to be an important consideration.

The fatigue properties of dentin have been studied in some detail, with reviews available in Refs. [15,16]. Human dentin is susceptible to fatigue failure (e.g. [17,18]) and small flaws

\* Corresponding author. Department of Mechanical Engineering, University of Maryland Baltimore County, 1000 Hilltop Circle, Baltimore, MD 21250, USA. Tel.: +1 410 455 3310; fax: +1 410 455 1052.

E-mail address: [darola@umbc.edu](mailto:darola@umbc.edu) (D.D. Arola).

<sup>1</sup> Shared equally in development of this manuscript and are co-first authors.

introduced via restorative processes may propagate via fatigue crack growth [19]. The resistance to fatigue and fatigue crack growth decreases with increasing proximity to the pulp [20], with increasing age of the patient [19,21,22], and with increasing mean stress [23] and stress ratio [24]. With resin composites becoming the predominant material for direct restorations, and their tendency to accumulate more biofilms than previous materials, the adjacent dentin is potentially more likely to undergo exposure to lactic acid produced by biofilms. Yet, no study has addressed the importance of acidic conditions to the fatigue properties of dentin.

In the present study we explore the influence of a clinically relevant acidic condition on the fatigue properties of human dentin. The overall objective was to evaluate the degradation in fatigue and fatigue crack growth resistance of this tissue with exposure to lactic acid.

## 2. Materials and methods

Caries-free third molars were obtained from participating dental practices in Maryland according to a protocol approved by the Institutional Review Board of the University of Maryland Baltimore County (Approval Y04DA23151). All teeth were from young individuals between 17 ≤ age ≤ 30 yrs. The teeth were maintained in Hanks Balanced Salt Solution (HBSS) with 0.2% sodium azide as an antimicrobial agent at 4 °C, then cast in a polyester resin foundation and sectioned using a computer controlled grinder (Chevalier Smart-H818II, Chevalier Machinery, Santa Fe Springs, CA, USA) and diamond impregnated slicing wheels (#320 mesh abrasives) under a water-based coolant bath. Primary sections were made in the bucco–lingual plane, and secondary sectioning was performed to obtain a rectangular beam or the body of a Compact Tension (CT) specimen from the coronal dentin (Fig. 1(a)). Rectangular beams were prepared from the mid-coronal space (midway between the DEJ and pulp) with geometry as described in Fig. 1(b). Similarly, the CT specimens were prepared according to the description of geometry in Fig. 1(c). The planar views of the specimens in Fig. 1(b) and (c) are consistent with the sectioned view of the specimens, and their preparations, in Fig. 1(a). For the CT specimens, additional features were needed, including two holes to permit application of the opening mode loads and a notch and back channel to facilitate crack initiation and extension. The notch was sharpened using a razor blade and diamond abrasive paste. Details concerning the preparations are described elsewhere [19,25]. Only one beam or CT specimen was obtained from each tooth. All of the prepared specimens were inspected via optical microscopy. Those identified as having pulp horn intrusions, enamel end-caps or other defects were discarded.

The dentin beams were subjected to 4-point flexure (Fig. 1(b)) using a universal testing system (BOSE Model ELF 3200, Minnetonka, MN, USA) with a load capacity and sensitivity of 225 N and ±0.01 N, respectively. Cyclic loading was conducted using a maximum load between roughly 5 and 15 N, a stress ratio ( $R = \text{min load}/\text{max load}$ ) of 0.1 and frequency of 5 Hz after previous studies [18,26]. According to the method of preparation, the dentin tubules were oriented perpendicular to the beam length and perpendicular to the direction of maximum principal stress caused by flexure loading. All of the flexure specimens were oriented with the pulpal side subjected to tension, and using cyclic loads that resulted in failures of 1k cycles or greater (i.e. the stress-life regime). For those beams that endured more than 1200k cycles, the test was discontinued as that is near the apparent endurance limit of dentin as identified in previous studies [18,26]. The fatigue life distribution of the specimens that underwent fatigue failure in each group was modeled using a Basquin-type power law model [27] according to

$$\sigma = A(N)^B \quad (1)$$

where  $A$  and  $B$  are the fatigue-life coefficient and exponent, respectively. The constants were obtained from a regression of the fatigue responses plotted on a log-normal scale. For the results obtained at pH = 5, alternate models were applied to the fatigue data and assessed in terms of the coefficient of determination. The apparent endurance limit was estimated from the models for a fatigue limit conveniently defined at  $1 \times 10^7$  cycles. This number is consistent with that identified in previous studies [18,25]. The control specimens ( $N = 75$ ) were subjected to cyclic loading within HBSS (pH = 7) at 22 °C, and consisted of a combination of previously reported data [26] and ten additional specimens. Cyclic loading of the treated specimens ( $N = 32$ ) was conducted within a lactic acid solution with pH = 5 at 22 °C. The fatigue strength distributions for the control (pH = 7) and treated (pH = 5) groups were compared over lives using the Wilcoxon Rank-Sum test with the critical value ( $\alpha$ ) set at 0.05.

The choice of conditions for acid exposure was based on a number of considerations. *Streptococcus mutans* (*S. mutans*), one of the most prevalent bacterial species in oral biofilms [28], metabolize fermentable carbohydrates to produce lactic acid [29]. *S. mutans* carry out glycolysis and maintain adhesion to the tooth surface down to pH of 4.5 [30,31]. Experimental evaluations of resin composites consider pH

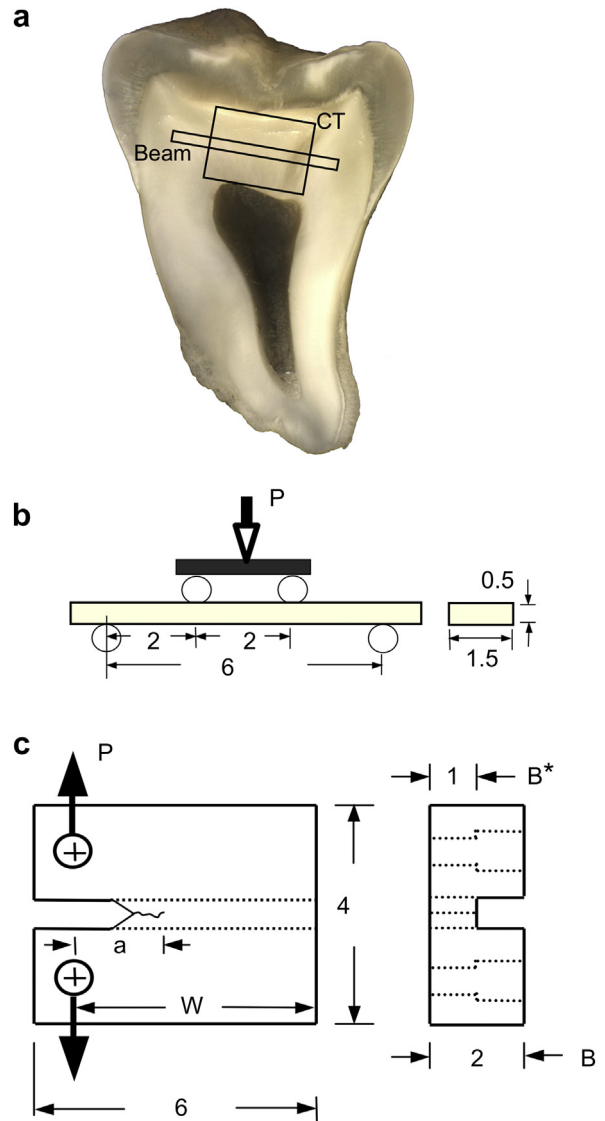


**Fig. 1.** Preparation of the specimens and method of loading. a) Potential Compact Tension (CT) and beam specimens from a sectioned 3rd molar. b) Flexure specimen geometry and loading configuration. The beams were arranged with the pulpal side subjected to compression. (c) CT specimen geometry and opening mode loading. By virtue of the methods of sectioning and cyclic loading, fatigue crack growth occurs perpendicular to the tubules. During cyclic loading of the rectangular beams the crack generated by stress-life fatigue develops and grows in plane and parallel to the length of the tubules.

values as low as 4 (e.g. [32,33]). A reduction below pH = 5.0 causes a disruption in the community of bacteria and its stability [28,34]. Thus, a lactic acid solution with pH = 5 was considered a clinically relevant model for evaluating the effects of acid conditions on the fatigue resistance of dentin. Nevertheless, this condition represents a simple static model, and cannot replace the complexity of conditions within the oral environment and the fluctuations in pH. The lactic acid solution was prepared by adding 7.45 ml of 0.1M lactic acid to 950 ml of deionized water. Then a basic solution of NaOH was added to the lactic acid solution until reaching the desired pH as verified with a pH meter (Model PH220-C, Extech, Waltham, MA, USA). Preliminary experiments were conducted to ensure that the pH of the lactic acid bath remained constant at pH = 5 despite dissolution of the mineral ions over the maximum duration of fatigue testing.

Cyclic loading of the CT specimens was performed with the aforementioned universal testing system using routine methods described elsewhere [19,25]. Briefly, the specimens were subjected to Mode I cyclic loading at 5 Hz frequency under load control as shown in Fig. 1(c). Cyclic loading was performed initially within HBSS using a stress ratio of 0.5 to facilitate crack initiation. After development of a sharp crack (length less than 0.5 mm), the HBSS was exchanged with the lactic acid solution and cyclic loading was continued using  $R = 0.1$  for cyclic crack growth. This

approach to lactic acid exposure ensured that all specimens were subjected to the same period of exposure at the inception of cyclic crack growth. The incremental crack growth rates ( $da/dN$ ) were computed by dividing the measured incremental crack extension ( $\Delta a$ ) by the increment of loading cycles ( $\Delta N$ ). Crack length measurements were achieved using a digital microscope (Navitar IEEE 1394, Rochester, NY, USA) at a magnification of 60 $\times$ . The number of cycles between measurements ( $\Delta N$ ) typically ranged between 5k and 20k cycles and was chosen according to the observed crack growth rate. The average crack extension over this period was between 60 and 120  $\mu\text{m}$ .

The incremental fatigue crack growth rate ( $da/dN$ ) within the region of steady state (Region II) response was quantified using the Paris Law [35] according to

$$\frac{da}{dN} = C(\Delta K)^m \quad (2)$$

where  $\Delta K$  is the stress intensity range, and the quantities  $C$  and  $m$  are the fatigue crack growth coefficient and exponent, respectively. The stress intensity range ( $\Delta K$ ) is the difference in stress intensity at the minimum and maximum loads and determined according to [19]

$$\Delta K_I = \frac{\Delta P}{B^* \sqrt{W}} \left( \frac{B^* + 1}{B + 1} \right)^{0.5} (0.131 + 0.320\alpha + 0.211\alpha^2) \quad (3)$$

where  $\Delta P$  is the load range ( $P_{\text{max}} - P_{\text{min}}$ ),  $\alpha$  is the ratio of  $a$  to  $W$  (Fig. 1(c)) and the quantities  $B^*$  and  $B$  are the ligament thickness and nominal specimen thickness, respectively. Using the incremental crack length measurements and the corresponding stress intensity, the fatigue crack growth rates ( $da/dN$ ) were plotted in terms of  $\Delta K$  to estimate the quantities  $C$  and  $m$  for each specimen. In addition, the apparent stress intensity threshold ( $\Delta K_{\text{th}}$ ) was estimated for a fatigue crack growth rate of  $1 \times 10^{-7}$  mm/cycle, which defines a critical stress intensity below which fatigue crack growth does not occur, or at a negligible rate. Similar to the stress-life fatigue analysis, the fatigue crack growth evaluation was conducted in two environmental conditions. The control ( $N = 32$ ) and treated ( $N = 6$ ) specimens were subjected to cyclic loading within HBSS (pH = 7) and lactic acid solution (pH = 5), respectively, at 22  $^{\circ}\text{C}$ . Results for the control group were also reported in Ivancik et al., [22]. The values of  $C$ ,  $m$  and  $\Delta K_{\text{th}}$  for the two groups were compared using a one-way Analysis of Variance with significant differences identified by  $p \leq 0.05$ . The fatigue crack growth distributions were compared using the Wilcoxon Rank-Sum test with the critical value ( $\alpha$ ) set at 0.05.

Acid exposure was expected to cause demineralization of the dentin specimens, and changes to the surface and sub-surface qualities. The external features of importance include the specimen geometry and surface topography, whereas the sub-surface features include the dentin tubule diameter and material hardness. All of the aforementioned qualities are potentially important to the fatigue properties of dentin. Therefore, the specimen dimensions and surface roughness were evaluated as a function of the period of cyclic loading. Details of the methods used for characterizing the specimen geometry and surface topography are listed in the Supporting Information (S1 and S2, respectively). Penetration of the lactic acid within the lumens over the period of cyclic loading could cause an increase in lumen diameter via demineralization. Thus, dimensional changes in the lumens were evaluated over the period of cyclic loading via microscopy using methods described in Supporting Information (S3). Furthermore, a reduction in elastic modulus of the intertubular dentin could occur, and was evaluated as a function of distance from the exposed surfaces using scanning based nanoindentation. Details regarding the methods used for evaluating changes to the sub-surface integrity with acid exposure are described in the Supporting Information (S4).

After fatigue failure the specimens were evaluated using a Scanning Electron Microscope (SEM; JSM 5600, JEOL Inc., Peabody, MA) in secondary electron imaging mode. Selected specimens were dehydrated in a standard ascending ethanol series (70–100%) and then sputtered with gold palladium. The fracture surfaces were examined to distinguish the origin of failure and contributing mechanisms.

### 3. Results

A fatigue life diagram for specimens evaluated within the lactic acid solution is shown in Fig. 2(a). The responses are presented initially in the “uncorrected” state, which represents the cyclic stress amplitude estimated from the specimen geometry at the beginning of cyclic loading. The lactic acid solution caused a reduction in the cross-section area of the specimens, and the degree of change increased over the period of exposure (Supporting Information S1; Fig. S1). The pulpal side underwent the largest extent of material loss overall. Thus, empirical models were developed to describe the change in specimen geometry in terms of the exposure period, and then used to correct the moment of inertia and the corresponding cyclic stress amplitude. The

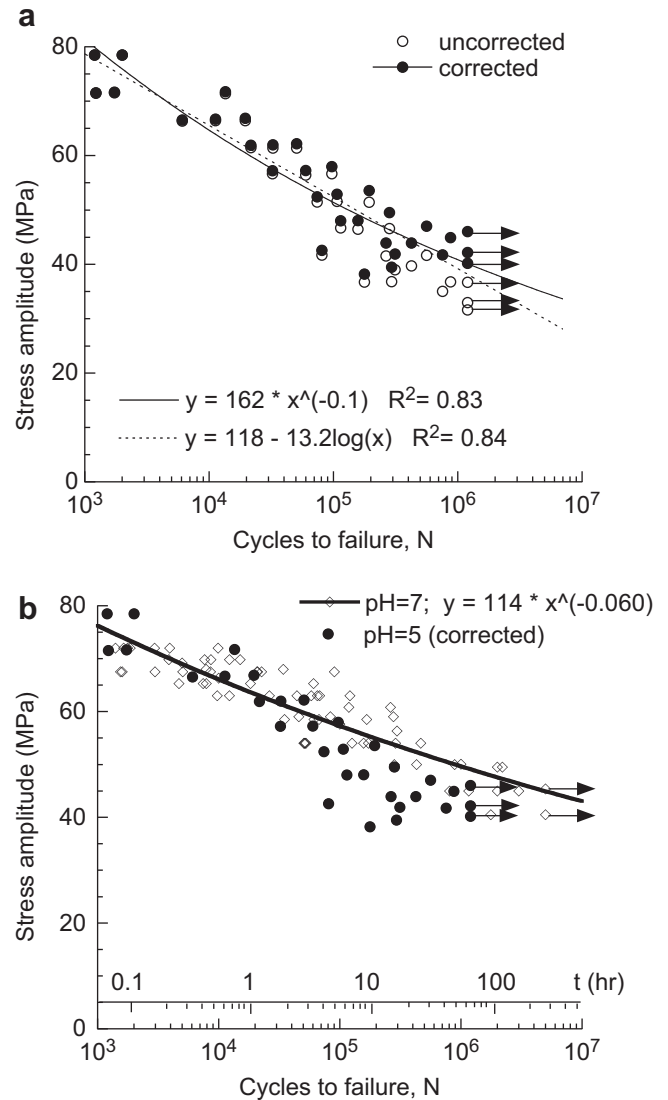


**Fig. 2.** Stress life fatigue behavior of the coronal dentin specimens. Each data point in these figures corresponds to failure of a single beam, and those with arrows identify beams that did not fail and the test was discontinued. (a) the stress-life responses for the treated specimens (pH = 5) before (uncorrected) and after correction for changes in the beam geometry that resulted from demineralization. Fatigue life models are presented for the distribution after correction. (b) A comparison of the fatigue life distributions for the control evaluated in HBSS (pH = 7) and the lactic acid solution (pH = 5). Note the reduction in fatigue life of the specimens subjected to lactic acid near 4 h of exposure and thereafter.

“corrected” fatigue life distribution, which accounts for changes in specimen geometry, is presented along with the uncorrected responses in Fig. 2(a). There is a change in the apparent fatigue strength distribution of the dentin specimens after accounting for material loss, which becomes more evident with increasing exposure, and especially after 100k cycles.

A conventional power law model was developed to describe the fatigue strength distribution of the corrected responses, and is presented along with the data in Fig. 2(a). Alternate models were considered for quantifying the corrected pH = 5 data. A logarithmic model exhibited the highest correlation to the corrected fatigue life distribution, as determined from the coefficient of determination ( $R^2$ ). Using the power law and logarithmic models of best fit, the apparent endurance limit of the dentin exposed to

lactic acid are 32 MPa and 26 MPa, respectively, when evaluated at  $1 \times 10^7$  cycles.

Results from experiments conducted in the lactic acid solution (pH = 5) are compared with the control specimens evaluated in HBSS (pH = 7) in Fig. 2(b). The number of cycles to failure decreased with an increase in cyclic stress for both pH conditions. For specimens that endured less than 50k cycles (approx. 3 h of cyclic loading), the fatigue strengths of specimens evaluated in lactic acid and HBSS are consistent. However, for lives exceeding this value the extended exposure to acid caused degradation of the fatigue strength in relation to that at pH = 7. According to the Wilcoxon Rank-Sum test, the fatigue strength distribution for the lactic acid treated specimens is significantly different ( $Z = -2.16$ ;  $p = 0.030$ ) from the control. Using the power law model developed for the fatigue responses (Fig. 2(b)), the apparent endurance strength of dentin evaluated within the control environment is 44 MPa. That value is more than 35% greater than the most liberal estimate for the apparent endurance limit of dentin at pH = 5.

Scanning electron microscopy was used to examine the fracture surfaces of specimens evaluated in the two conditions. All of the specimens exhibited similar macroscopic features, regardless of the loading environment. The fracture surface of a specimen evaluated within the lactic acid solution is shown in Fig. 3(a). Evident here, failure initiated on the tensile side as distinguished by the compression curl (C). Though not possible to identify the origin of failure, it was apparent that a crack developed on the tensile side and extended parallel to the tubules until reaching the compressive side of the neutral axis. Thereafter, the crack turned oblique and proceeded to enable fracture of the specimen, consistent with earlier studies [18,26]. At higher magnification there were some differences in the fracture surfaces between the two groups of specimens. In examining the tensile surface of a beam evaluated with pH = 5 (Fig. 3(b)), cracks are evident within the partially

demineralized peritubular cuffs, and there are exposed collagen fibrils (arrows). These features suggest that lactic acid penetrated beneath the specimen's surface, causing demineralization of the cuff and reduction in fatigue strength. A micrograph from the fracture surface of a control specimen at high magnification is shown in Fig. 3(c). Note that the tubule lumens are evident, but there are no cracks along the peritubular cuffs or exposed collagen fibrils.

The fatigue crack growth responses for specimens evaluated in lactic acid and HBSS are presented in Fig. 4. A comparison of representative responses along with the power law fit to the data is shown in Fig. 4(a). The cumulative responses for all specimens of the two groups are shown in Fig. 4(b). A correction for changes in geometry was not necessary as the contribution to the estimated stress intensity range (Eq. (3)) over the period of exposure was negligible. Similar to the stress-life fatigue responses, the exposure to lactic acid caused a decrease in the fatigue crack growth resistance of dentin. According to the Wilcoxon Rank-Sum Test the two fatigue crack growth distributions are significantly different ( $Z = -2.41$ ;  $p = 0.016$ ). Cyclic crack growth in the lactic acid solution initiated at a significantly lower ( $p < 0.0005$ ) stress intensity range ( $\Delta K_{th} \approx 0.71 \text{ MPa m}^{0.5}$ ) than in HBSS ( $\Delta K_{th} \approx 0.83 \text{ MPa m}^{0.5}$ ). Stable cyclic crack growth within Region II of the responses (Fig. 3) was characterized using the Paris Law according to Eq. (2) and the average values for the two groups are presented in Table 1. There was an increase in the fatigue crack growth exponent from  $14 \pm 2$  in HBSS to  $26 \pm 4$  in lactic acid, suggesting that the reduction in pH caused an increase in sensitivity to the stress intensity range. Overall, there was a significant difference ( $p \leq 0.05$ ) in all three of the fatigue crack growth parameters (Table 1) between results obtained at pH = 5 and pH = 7. Nevertheless, an SEM evaluation of the fracture surfaces did not reveal any differences between the specimens loaded in HBSS and lactic acid. Although there was some

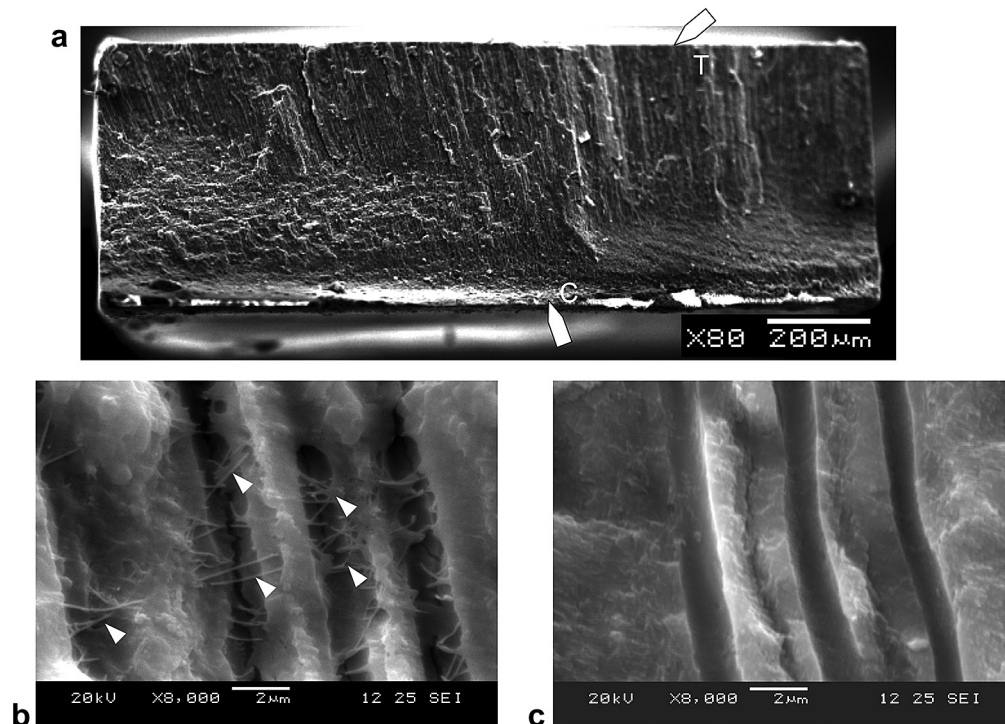


**Fig. 3.** Micrographs of a fractured dentin specimen after fatigue loading to failure in the lactic acid solution. a) the fracture surface of a dentin beam after  $5 \times 10^5$  cycles. This specimen was subjected to a cyclic stress amplitude of 40 MPa. The tensile surface (T) and compression curl (C) are highlighted. b) Micrograph from the specimen in (a) near the tensile surface and at higher magnification ( $\times 8000$ ) revealing collagen fibrils (arrows) exposed on the fracture surface. c) a high magnification photo of a control specimen for comparison to (b). Note that absence of collagen fibrils, which are clearly evident in (b).

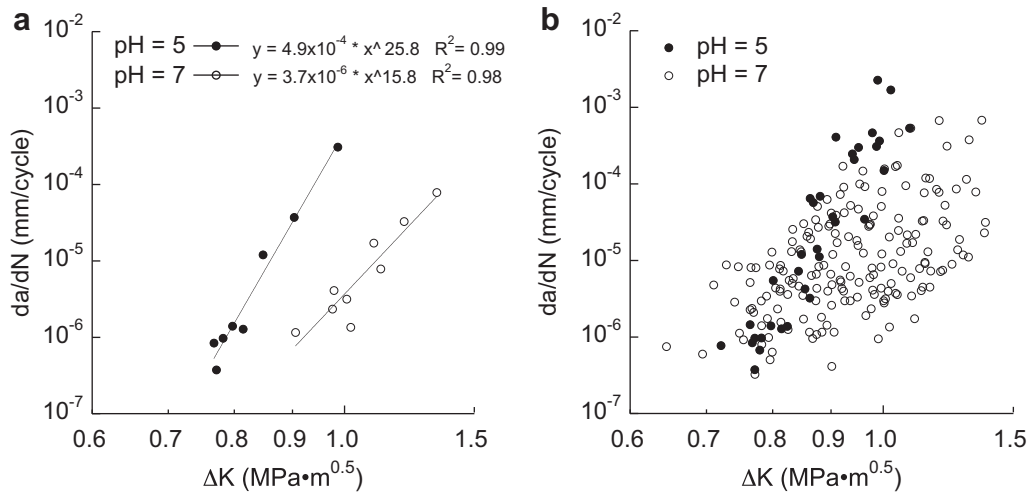


**Fig. 4.** A comparison of the fatigue crack growth responses of coronal dentin in HBSS (pH = 7) and lactic acid solution (pH = 5). a) Representative responses with corresponding power law fit for both pH conditions. b) The responses obtained for all of the control ( $N = 32$ ) and treated ( $N = 6$ ) specimens. Note the reduction in fatigue crack growth resistance of the tissue with exposure to lactic acid.

evidence of demineralization to the exterior surfaces and exposed crack face of the specimens, there were no indication that exposure to lactic acid changed the mechanisms of cyclic crack growth.

There was a significant reduction to both the fatigue strength and fatigue crack growth resistance of the coronal dentin with exposure to lactic acid. That could result from focused demineralization at the surface, or by penetration and more extensive sub-surface degradation. A smear layer covered the control specimens and remained intact on those that underwent relatively short periods of acid exposure. That is a common characteristic observed after cutting of dentin [36]. However, after longer periods of acid exposure (e.g. 100k cycles and greater) the tubules became exposed at the surface of specimens via demineralization of the smear plugs within the lumens (Fig. 5(a)). There were also affects of acid exposure to the surface topography. A comparison of surface profiles obtained before cyclic loading and after 1 million cycles of loading in lactic acid is shown in Fig. 5(b)). The average surface roughness ( $R_a$ ) increased with cyclic loading in the acid solution (Supporting Information S2; Fig. S2(a)), and was significantly greater ( $p \leq 0.05$ ) than that of the control after 100k cycles and beyond. That statement is equally true for measures of the peak to valley height ( $R_y$ ) and the ten point height ( $R_z$ ) as well. Dominant valleys of the profiles were examined as they can pose a surface stress concentration. An example profile radius for a valley in the profile of Fig. 5(b) is shown in Fig. 5(c). There was no apparent change in the profile valley radii resulting from the acid exposure, with values ranging between roughly 20 and 50  $\mu\text{m}$  (average  $35 \pm 13 \mu\text{m}$ ). Using the measures of roughness and profile valley radii, the effective stress concentration posed by the surface

topography (Supporting Information S2) ranged between 1.00 for the control surfaces to 1.03 after 1 million cycles of loading in the lactic acid solution. Therefore, there was no significant increase in the effective stress concentration at pH = 5 with period of cyclic loading, despite the increase in surface roughness.

According to the changes in observed surface morphology of the fatigue specimens, lactic acid penetrated within the lumens and beneath the exposed surface. The depth of degradation was undoubtedly dependent on the period of cyclic loading. The sub-surface characteristics of the microstructure for fatigue specimens subjected to 1k cycles and one million cycles of loading are shown in Fig. 6(a) and (b), respectively. Although there was limited evidence of sub-surface demineralization for periods of less than 1k cycles (e.g. Fig. 6(a)), those specimens subjected to 100k cycles and greater exhibited notable dissolution of the peritubular cuff, as evident in Fig. 6(b). In addition, many of the peritubular cuffs exhibited cracks within the partially demineralized region, as highlighted in this figure. That was also noted in the demineralized regions of the fracture surfaces for the acid-exposed specimens (Fig. 3(b)). The average depth of degradation is shown as a function of the period of exposure in Fig. 6(c). Beyond 10k cycles there was a significant ( $p < 0.000$ ) increase in the depth of degradation, with maximum depth occurring in the specimens subjected to one million cycles and extending up to 40  $\mu\text{m}$  from the surface.

Scanning probe microscopy was conducted to quantify the extent of sub-surface degradation in the intertubular dentin that resulted from cyclic loading within the lactic acid solution. Maps of the complex modulus distribution were obtained and used to determine the reduction in complex modulus adjacent to the acid-exposed surface (Supporting Information S4: Fig. S3). A representative complex modulus distribution is plotted in Fig. 7 in terms of distance from the tensile surface exposed to lactic acid. Each data point represents the complex modulus obtained along three unique paths (avoiding the peritubular cuffs) beginning from the acid-exposed surface and extending sub-surface a distance of 50  $\mu\text{m}$ . For the control condition (not exposed to acid), only the average and standard deviation in complex modulus are plotted for this condition (in green). The reduction in elastic modulus of the intertubular dentin caused by acid exposure is clearly apparent. As evident from the values near the exposed surface in Fig. 7, the depth of degradation extends to approximately 25  $\mu\text{m}$ , with values ranging between 25  $\mu\text{m}$  and 30  $\mu\text{m}$  for all the specimens evaluated

**Table 1**

A comparison of the fatigue crack growth parameters resulting from cyclic crack extension in the environments. The numerical values of the parameters listed for both conditions represent the average and standard deviation obtained from results of the individual specimens evaluated in HBSS ( $N = 32$ ) and lactic acid ( $N = 6$ ). In comparing results for pH = 5 and pH = 7, all three of the fatigue crack growth parameters were significantly different ( $p \leq 0.05$ ).

Condition	$\Delta K_{th}$ (MPa $\text{m}^{0.5}$ )	$C$ (mm/cycle) (MPa $\text{m}^{0.5}$ ) <sup>-<math>m</math></sup>	$m$
HBSS ( $N = 32$ )	$0.83 \pm 0.11$	$2.7 \text{ E}-05$	$14 \pm 2$
Lactic acid ( $N = 6$ )	$0.71 \pm 0.03$	$6.6 \text{ E}-04$	$26 \pm 4$
	$p = 0.016$	$p = 0.0005$	$p = 0.0005$

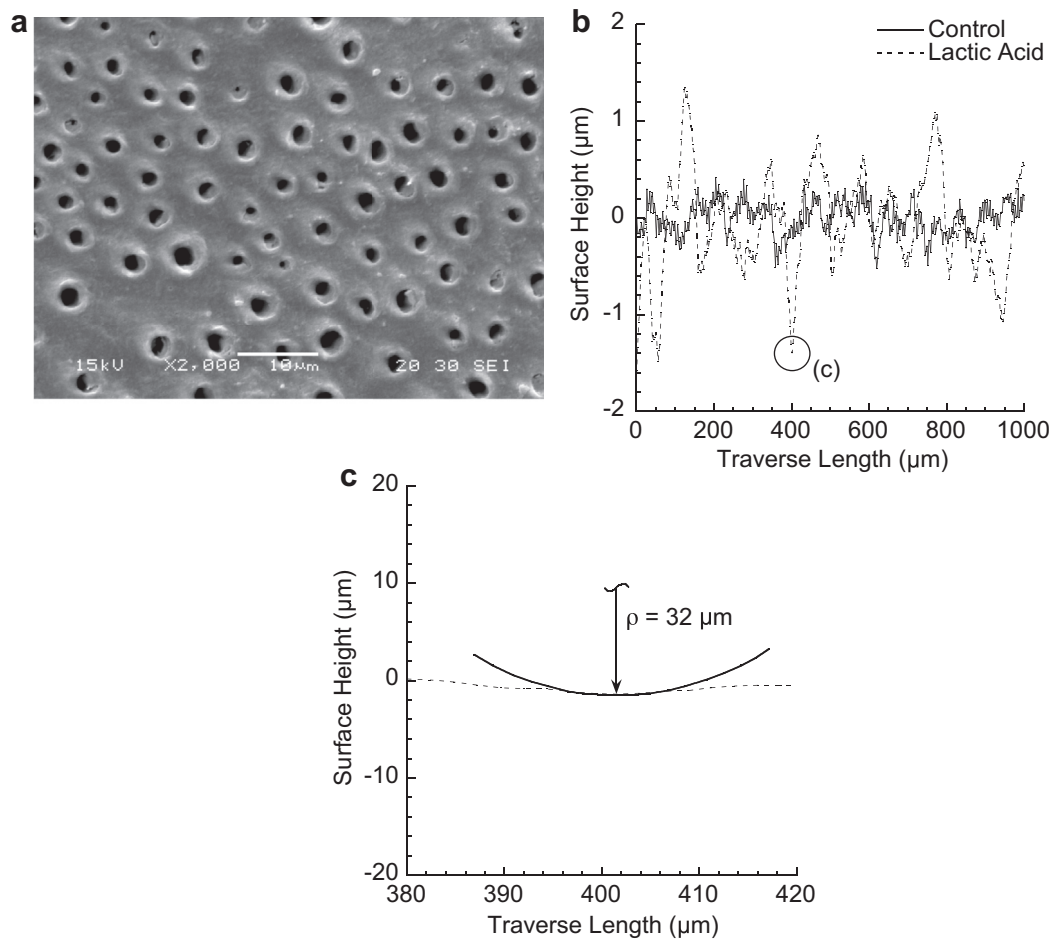


**Fig. 5.** Surface characteristics of the dentin specimens before and after cyclic loading. a) Micrograph obtained from the tensile surface of dentin specimens evaluated in lactic acid after 1 million cycles. Note the open lumens evident on this surface, which are generally covered by a smear layer. b) Comparison of the surface topography of a specimen before cyclic loading (control) and a specimen evaluated in lactic acid after 1 million cycles of loading. c) Profile valley from (b) with measure of the valley radius of curvature.

that reached one million cycles. The depth of apparent degradation in modulus is in agreement with the penetration noted in demineralization of the peritubular cuffs (Fig. 6(c)).

#### 4. Discussion

Secondary caries at the tooth margin are the most common cause of restoration failure and result from the acid production of biofilms [6,37,38]. A local plaque pH of above 6 is the safe zone, a pH of 6.0 to 5.5 is potentially cariogenic, and between 5.5 and 4 is the cariogenic or danger zone [39]. *In vitro* acidic solutions with pH of between 4 and 5 have been adopted to simulate *in vivo* acidogenic environments, and to evaluate the effectiveness of dental materials in maintaining mineralization of tooth tissue (e.g. [32,40,41]). Despite the clinical relevance of degradation to the mechanical properties of tooth tissues by acidic conditions, this is the first reported investigation to evaluate the fatigue properties of dentin at  $\text{pH} < 7$ . Overall, both the fatigue strength and fatigue crack growth resistance of coronal dentin underwent degradation at  $\text{pH} = 5$ .

Exposure of dentin to the lactic acidic solution resulted in a significant reduction in fatigue strength, with an apparent endurance limit of 32 MPa. That was nearly 30% lower than the apparent endurance limit of dentin within the control conditions (44 MPa). The comparison of fatigue responses presented in Fig. 2 conveys the importance of lactic acid exposure to both the finite-life fatigue behavior and the definition of the fatigue limit. For comparatively

short periods of cyclic loading (i.e.  $N_f \leq 50\text{k}$  cycles), the fatigue strength was not affected by the lactic acid, despite small changes in the specimen geometry (Supporting Information; Fig. S1). Beyond that duration of loading the changes in geometry were apparent and the affects of correction were important (Fig. 2(a)). Reported studies by Staninec et al., [42] and Mishra et al. [43,44] have discussed demineralization of dentin subjected to cyclic loading within acidic conditions and noted changes in specimen dimensions. However, in the present investigation there were additional aspects of degradation identified that further reduced the fatigue strength. These factors became evident after approximately 4 h of exposure (Fig. 2(b)). A quantitative description of this degradation was achieved by taking the difference between the mean fatigue strength distributions of the control and acid treated specimens, and treating this residual error using a least squares approach. That enabled development of an empirical model for the fatigue responses in terms of the sum of the “true fatigue” response caused by cyclic loading (i.e. of the control), and the degradation attributed to acid exposure. The newly developed model is compared with the experimental data in Fig. 8. From this presentation it is apparent that acid exposure causes a reduction in fatigue strength, and the extent of degradation caused by the acidic condition increases with time of exposure.

Although the model presented in Fig. 8 accounts for the superposed affects of mechanical fatigue and degradation by acid, it is important to emphasize that the model is not a constitutive model.

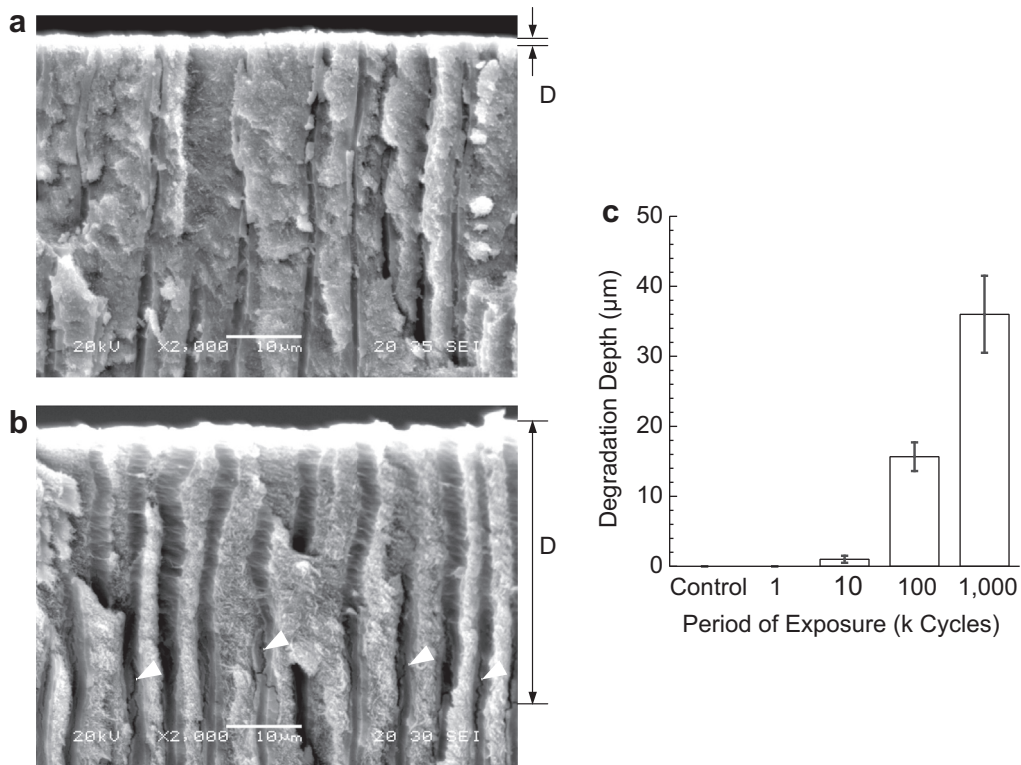


**Fig. 6.** Quantifying the depth of penetration of lactic acid within the dentin tubules and beneath the exposed surface. The depth of degradation (D) is identified in the micrographs of (a) and (b). a) Representative micrograph of the microstructure beneath the tensile surface of a beam after 1k cycles. b) Representative micrograph of the microstructure beneath the tensile surface of a beam after one million cycles of loading. Note the cracks within the partially demineralized tubule lumens (white arrows). c) Average depth of degradation (with standard deviation) assessed over different periods of evaluation.

It is essentially the “best-fit” of an empirical relationship to the experimental results that were obtained from specific conditions of evaluation. Changes to the environmental pH or the frequency of loading would likely reduce the effectiveness of this model for predicting the fatigue response. Even in application of the newly

developed model to predicting fatigue in the coronal dentin at pH = 5, not all the data is consistent with the prediction. Indeed, there is a large degree of scatter in the experimental data generated in the acidic conditions, and the degree of scatter increases with the period of acid exposure. This variability in the fatigue responses is believed to result from variations in the microstructure of dentin, and its importance to the rate of degradation with reduction in pH. Although the methods of sectioning were selected to obtain

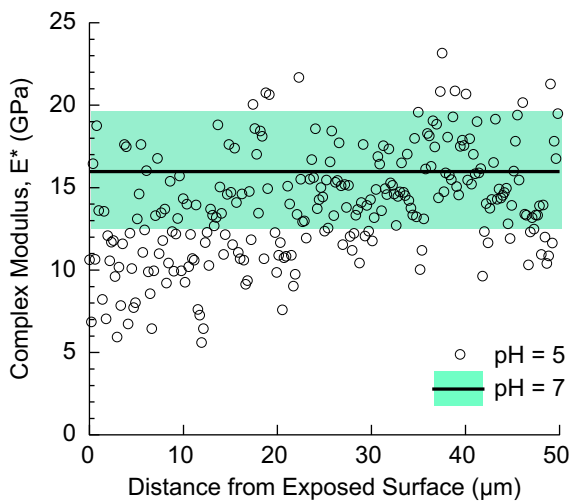


**Fig. 7.** Degradation in the complex modulus of dentin resulting from exposure to lactic acid. The complex modulus distribution is plotted as a function of distance across the modulus map. For the pH = 5 condition, the bottom surface (at x = 0) represents the surface exposed to lactic acid and subjected to cyclic tensile stress. The control condition represents the complex modulus for a map taken from the center of the specimen (not subjected to acid) and is plotted in terms of the average (line) and std dev. (green) of the complex modulus. (For interpretation of the references to color in this figure legend, the reader is referred to the web version of this article.)

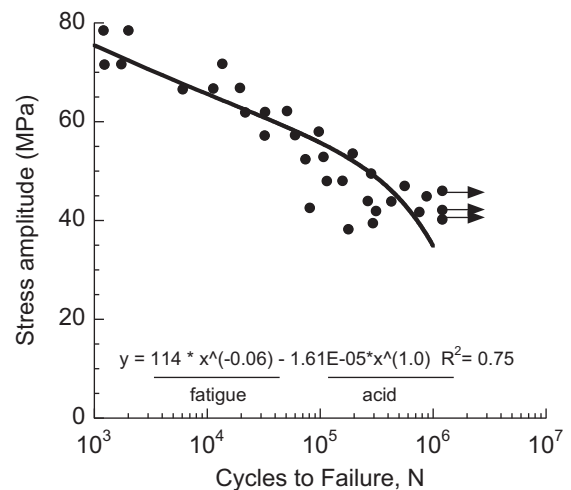


**Fig. 8.** Stress life fatigue behavior of the coronal dentin specimens evaluated in lactic acid and comparison with empirical model describing the responses in terms of the effects of fatigue and degradation by acid. The data points with arrows represent specimens that did not fail and the test was discontinued.

specimens with consistent microstructure, there were variations as evident from comparing the lumen density of Fig. 6(a) and (b). That observation suggests that a reduction in pH could be more detrimental to the fatigue behavior of dentin in other areas of the tooth, which warrants further investigation.

The question that remains to be answered regarding the reduction in fatigue resistance is “what were the predominant mechanisms of degradation?” Clearly there was a loss of mineral at the exposed surfaces that was noted from the removal of the smear plugs within the lumens (Fig. 4(a)) and as quantified from the changes in surface topography (Fig. 4(b)). That was also evident from the significant increase in measures of surface roughness (Supporting Information S2: Fig. S2) with exposure. The changes in roughness noted here were much greater than those reported to occur in exposure of resin composites to *S. mutans*, even after longer times periods [10]. Nevertheless, there was not a notable change in the profile valley radii that resulted from the lactic acid exposure (Fig. 3(c)). Despite the increase in surface roughness there was no significant increase in the degree of apparent stress concentration. Therefore, the degradation in fatigue resistance does not largely result from changes to the surface of the specimens.

Continuing to the sub-surface qualities, there was a progression of degradation beneath the exposed surfaces that was viewed by demineralization of the peritubular cuffs and an enlargement of the tubule diameter (Fig. 6(b)). Beyond 10k cycles of loading the depth of degradation increased significantly (Fig. 6(c)). The lumens do pose a stress concentration by virtue of their circular geometry, and that is important to fracture processes in this tissue [45,46]. But enlarging of the cuffs via demineralization does not necessarily increase the magnitude of the stress concentration; the nominal stress concentration factor for a circular hole is 3 regardless of the size of the hole [47]. But the increase in lumen diameter does equate to an increase in near-surface porosity. Perhaps a non-uniform and closely packed group of lumens can assemble to form a distributed stress concentration, and demineralization of the peritubular cuffs causes development of larger scale voids. That comment is speculative as a fractographic evaluation of the specimens did not reveal any origins of this type. There is a complementary form of demineralization to the intertubular dentin. The nanoDMA evaluation (Fig. 7) showed that prolonged cyclic loading within the lactic acid caused a reduction in elastic modulus and strength. Reviewing the aforementioned mechanisms, the lactic acid caused focused demineralization at the surfaces, which facilitated the fatigue process via reduction in mineral crystals. Progression of the demineralization caused an increase in sub-surface porosity, which results in loss of stiffness and corresponding increase in surface strains under flexure, both of which accelerated the process of fatigue. While there were changes in surface topography, they do not appear to be the most critical to the fatigue resistance.

Fracture has been identified as one of the three primary reasons for restored tooth failure [1,4,5]. Clinical assessments of these failures typically characterize the performance in terms of the life or duration of survival after placement. Consequently, it may be more clinically relevant to interpret the effects of lactic acid exposure in terms of fatigue life rather than strength. Here we choose to focus on the responses with cyclic stress amplitude between 30 and 50 MPa (Fig. 2(b)), which corresponds to fatigue lives equating to years of clinical function, assuming that normal occlusion bears 250k cycles/year or greater [48]. Within this region of stress amplitude the fatigue life of dentin exposed to lactic acid was as low as a tenth of the life achieved in HBSS. What may be more noteworthy is that the reduction in fatigue life begins after only 4 h of exposure (Fig. 2(b)). Thus, in the presence of lactic acid, tooth fractures may only be partly dependent on the magnitude of cyclic

stress. The success of a patient's oral hygiene and the armamentarium used in preventing acidic degradation could be considered important defenses to tooth fractures. Of potentially equal concern, most sports and energy drinks have pH values that are well below that of the lactic acid (pH = 5) used in this investigation [49]. Therefore, while a reduction in pH may be important to dental erosion [50], an individual's diet may have additional detrimental effects and be a relevant concern in the failing of tooth structure by fatigue and fracture.

Admittedly, a reduction in the fatigue strength of dentin with exposure to lactic acid was expected. But considering the mechanics of crack opening in the lactic acid solution, the expected effects on fatigue crack growth were not clear. Localized demineralization at the initiated crack tip could initiate blunting and a consequent reduction in the local stress intensity available to drive crack extension. Conversely, demineralization could reduce the intrinsic toughness of the tissue and effectiveness of the toughening mechanisms. The ligament bridges are the most potent extrinsic mechanism contributing to the toughness of dentin [46] and demineralization of the bridging ligaments would reduce their strength, thereby facilitating accelerated cyclic extension. But the fatigue crack growth responses (Fig. 4) showed that the lactic acid solution contributed to both the initiation and steady-state aspects of cyclic extension. Specifically, there was a reduction in the threshold stress intensity range ( $\Delta K_{th}$ ) necessary to initiate cyclic extension, and an increase in sensitivity to the stress intensity range as noted by the increase in  $m$  (Table 1). When the responses in Fig. 4 are compared in terms of the average fatigue crack growth rates, the reduction in pH caused an increase in the incremental rate of extension of between 2 and 10 times that of the control. That equates to a fatigue life of between one half and one tenth of that in neutral conditions. As fatigue crack growth is generally a precursor to unstable fracture, exposure of dentin to lactic acid substantially increases the likelihood of restored tooth failure by fracture.

The objective of this investigation was to explore the influence of exposure to lactic acid on the fatigue properties of dentin. Though the lactic acid condition may be considered as a simple model for the acid produced by biofilms, there are added complexities involved in the exposure of tooth structure to biofilms that serves as a limitation of this investigation. There are some additional limitations as well. Perhaps the most relevant is the choice of cyclic loading conditions used for the fatigue experiments. Cyclic loading was conducted at 22 °C and with continuous exposure to a lactic acid solution maintained at a constant pH. Many aspects of the daily routine, along with diffusion, would cause fluctuations in pH and temperature. It is unlikely that the local oral environment of dentin would be maintained at a constant pH of 5. Nevertheless, *S. mutans* can survive and carry out glycolysis over a range of pH values, down to 4 and lower [51]. While the effects of neutralization resulting from oral functions are important, it is equally possible that the localized conditions could reach pH values less than 5 [28,34]. Environments with higher pH levels may require more time for degradation to take place, but the consequences would be equally detrimental.

The format used for fatigue testing of the dentin specimens may raise concern. Flexure loading amplifies the effects from demineralization due to the development of maximum stress at the surface where acid concentration is greatest. Indeed, the reduction in apparent fatigue strength caused by pH variations would be expected to be greater in flexure than uniaxial tension. Yet finite element studies have shown that stress gradients are common at the bonded interface of restored teeth [52,53] and uniaxial tension at the bonded interface is rare. Hence, the stress distribution is arguably a clinically relevant format for evaluation. In addition, cyclic loading was conducted at 5 Hz, which is up to four times

faster than typical values associated with mastication [54]. The fatigue strength of dentin increases with frequency [17,55]. Utilizing a higher frequency can promote accelerated degradation by true “fatigue”, which may reduce the relative effects of demineralization on the fatigue response over time, ignoring the potential for synergism between fatigue and demineralization. Lastly, an apparent endurance limit of  $1 \times 10^7$  cycles was adopted for comparing the fatigue responses after the definition used in previous investigations [18,26]. With an estimated 500 to 750k cycles of mastication per year [48], the aforementioned definition corresponds to 15–20 years of oral function. It is not known whether dentin exhibits a true endurance limit (e.g. akin to steels), as that value could be influenced by a myriad of oral conditions *in vivo*. Thus, the use of  $1 \times 10^7$  cycles should be considered a basis for comparison and figure of merit, but not the lifetime of teeth. Equally important, the power law models used for estimating the apparent endurance limits were adopted to maintain consistency in the definition of fatigue behavior. Alternate models could be used and would likely influence the “quantitative” description of the degradation caused by acid exposure.

Despite the aforementioned concerns, this study has shown for the first time that exposure of dentin to acidic conditions results in a significant reduction in resistance to fatigue failures. This degradation in fatigue properties raises some concern regarding the effects from acid etching (e.g. in the placement of resin composites) on the fatigue resistance of the supporting dentin. Filling the tooth cavity with restorative materials having capacity for acid-neutralization [56], and the use antibacterial bonding agents for disarming biofilm at the margins [57,58] are appearing more essential, not only for reducing the incidence of secondary caries, but also for decreasing the likelihood of fatigue related failures.

## 5. Conclusions

On the basis of the results obtained, the following conclusions may be drawn;

- 1) In comparing the stress-life fatigue behavior of coronal dentin in solutions with pH = 7 (HBSS, control) and pH = 5 (lactic acid), the acidic environment resulted in a significant reduction ( $p \leq 0.05$ ) in the resistance to fatigue failure. The apparent endurance limit of dentin in the lactic acid solution was 32 MPa and nearly 30% lower than that of the control (44 MPa). When characterized as a function of time, the reduction in fatigue strength developed after only 4 h of exposure to lactic acid solution with pH = 5.
- 2) There was a significant reduction ( $p \leq 0.05$ ) in the fatigue crack growth resistance of dentin when subjected to the lactic acid environment. Exposure to lactic acid caused a 15% reduction in the critical stress intensity range necessary for the initiation of cyclic extension, and up to 10 fold increase in the rate of incremental crack growth when compared to the control conditions.
- 3) The lactic acid solution caused at least three different forms of microstructural degradation that contributed to the decrease in fatigue resistance, including i) loss of mineral at the exposed surfaces and an increase in surface roughness, ii) demineralization of the peritubular dentin causing enlargement of the tubule diameter, and iii) demineralization of the intertubular dentin causing reduction in elastic modulus and strength. The second and third mechanisms are the most detrimental. If dentin is exposed to lactic acid via biofilms, prolonged exposure without remineralization will increase the likelihood of restored tooth failure by fatigue and potentially facilitate tooth fracture.

## Acknowledgments

This study was supported in part by grant NIH R01 DE016904 (PI. D. Arola) from the National Institute of Dental and Craniofacial Research (NIDCR) and by matching seed grants from the University of Maryland Baltimore County and University of Maryland, Baltimore (H.H.K. Xu and D. Arola).

## Appendix A. Supplementary data

Supplementary data related to this article can be found at <http://dx.doi.org/10.1016/j.biomaterials.2013.07.090>.

## References

- [1] Ferracane JL. Resin composite-state of the art. *Dent Mater* 2011;27(1):29–38.
- [2] Bernardo M, Luis H, Martin MD, Leroux BG, Rue T, Leitão J, et al. Survival and reasons for failure of amalgam versus composite posterior restorations placed in a randomized clinical trial. *J Am Dent Assoc* 2007;138(6):775–83.
- [3] Demarco FF, Corrêa MB, Cenci MS, Moraes RR, Opdam NJ. Longevity of posterior composite restorations: not only a matter of materials. *Dent Mater* 2012;28(1):87–101.
- [4] Mjor IA, Toffenetti F. Secondary caries: a literature review with caries reports. *Quintessence Int* 2000;31(3):165–79.
- [5] Sarrett DC. Clinical challenges and the relevance of materials testing for posterior composite restorations. *Dent Mater* 2005;21(1):9–20.
- [6] Sakaguchi RL. Review of the current status and challenges for dental posterior restorative composites: clinical, chemistry, and physical behavior considerations. *Dent Mater* 2005;21(1):3–6.
- [7] Ten Cate JM. Biofilms, a new approach to the microbiology of dental plaque. *Odontology* 2006;94(1):1–9.
- [8] Zalkind MM, Keisar O, Ever-Hadani P, Grinberg R, Sela MN. Accumulation of *Streptococcus mutans* on light-cured composites and amalgam: an in vitro study. *J Esthet Dent* 1998;10(4):187–90.
- [9] Beyth N, Domb AJ, Weiss EI. An in vitro quantitative antibacterial analysis of amalgam and composite resins. *J Dent* 2007;35(3):201–6.
- [10] Beyth N, Bahir R, Matalon S, Domb AJ, Weiss EI. *Streptococcus mutans* biofilm changes surface-topography of resin composites. *Dent Mater* 2008;24(6):732–6.
- [11] Fúcio SB, Carvalho FG, Sobrinho LC, Sinhoretí MA, Puppim-Rontani RM. The influence of 30-day-old *Streptococcus mutans* biofilm on the surface of esthetic restorative materials—an in vitro study. *J Dent* 2008;36(10):833–9.
- [12] Busscher HJ, Rinastiti M, Siswomihardjo W, Van Der Mei HC. Biofilm formation on dental restorative and implant materials. *J Dent Res* 2010;89(7):657–65.
- [13] Marshall Jr GW, Marshall SJ, Kinney JH, Balooch M. The dentin substrate: structure and properties related to bonding. *J Dent* 1997;25(6):441–58.
- [14] Kinney JH, Marshall SJ, Marshall GW. The mechanical properties of human dentin: a critical review and re-evaluation of the dental literature. *Crit Rev Oral Biol Med* 2003;14(1):13–29.
- [15] Kruzic JJ, Ritchie RO. Fatigue of mineralized tissues: cortical bone and dentin. *J Mech Behav Biomed Mater* 2008;1(1):3–17.
- [16] Arola D, Bajaj D, Ivancik J, Majd H, Zhang D. Fatigue of biomaterials: hard tissues. *Int J Fatigue* 2010;32(9):1400–12.
- [17] Nalla RK, Imbeni V, Kinney JH, Staninec M, Marshall SJ, Ritchie RO. In vitro fatigue behavior of human dentin with implications for life prediction. *J Biomed Mater Res* 2003;66(1):10–20.
- [18] Arola D, Reprogl R. Effects of aging on the mechanical behavior of human dentin. *Biomaterials* 2005;26(18):4051–61.
- [19] Bajaj D, Nazari A, Sundaram N, Arola D. Aging, dehydration and fatigue crack growth in human dentin. *Biomaterials* 2006;27(11):2507–17.
- [20] Ivancik J, Neerchal NK, Romberg E, Arola D. On the reduction in fatigue crack growth resistance of dentin with depth. *J Dent Res* 2011;90(8):1031–6.
- [21] Kinney JH, Nalla RK, Pople JA, Breunig TM, Ritchie RO. Age-related transparent root dentin: mineral concentration, crystallite size, and mechanical properties. *Biomaterials* 2005;26(16):3363–76.
- [22] Ivancik J, Majd H, Bajaj D, Romberg E, Arola D. Contributions of aging to the fatigue crack growth resistance of human dentin. *Acta Biomaterialia* 2012;8(7):2737–46.
- [23] Nalla RK, Kinney JH, Marshall SJ, Ritchie RO. On the in vitro fatigue behavior of human dentin: effect of mean stress. *J Dent Res* 2004;83(3):211–5.
- [24] Arola D, Zheng W, Sundaram N, Rouland JA. Stress ratio contributes to fatigue crack growth in dentin. *J Biomed Mater Res A* 2005;73(2):201–12.
- [25] Zhang D, Nazari A, Soappman M, Bajaj D, Arola D. Methods for examining the fatigue and fracture behavior of hard tissues. *Exp Mechanics* 2007;47(3):325–36.
- [26] Arola D, Reprogl R. Tubule orientation and the fatigue strength of human dentin. *Biomaterials* 2006;27(9):2131–40.
- [27] Stephens RI, Fatemi A, Stephens RR, Fuchs HO. *Metal fatigue in engineering*. 2nd ed. New York: John Wiley and Sons, Inc; 2001.

- [28] Kolenbrander PE. Oral microbial communities: biofilms, interactions, and genetic systems. *Annu Rev Microbiol* 2000;54:413–37.
- [29] Clarke JK. On the bacterial factor in the aetiology of dental caries. *Br J Exp Pathol* 1924;5(3):141–6.
- [30] Padan E, Zilberstein D, Schuldiner S. pH homeostasis in bacteria. *Biochim Biophys Acta* 1981;650(2–3):151–66.
- [31] Drobni M, Li T, Krüger C, Loimaranta V, Kilian M, Hammarström L, et al. Host-derived pentapeptide affecting adhesion, proliferation, and local pH in biofilm communities composed of *Streptococcus* and *Actinomyces* species. *Infect Immun* 2006;74(11):6293–9.
- [32] Xu HH, Moreau JL, Sun L, Chow LC. Nanocomposite containing amorphous calcium phosphate nanoparticles for caries inhibition. *Dent Mater* 2011;27(8):762–9.
- [33] Weir MD, Chow LC, Xu HH. Remineralization of demineralized enamel via calcium phosphate nanocomposite. *J Dent Res* 2012;91(10):979–84.
- [34] Bradshaw DJ, Marsh PD. Analysis of pH-driven disruption of oral microbial communities in vitro. *Caries Res* 1998;32(6):456–62.
- [35] Paris PC, Gomez MP, Anderson WP. A rational analytic theory of fatigue. *Trend Eng* 1961;13:9–14.
- [36] Banerjee A, Kidd EA, Watson TF. Scanning electron microscopic observations of human dentine after mechanical caries excavation. *J Dent* 2000;28(3):179–86.
- [37] Deligeorgi V, Mjor IA, Wilson NH. An overview of reasons for the placement and replacement of restorations. *Prim Dent Care* 2001;8(1):5–11.
- [38] Featherstone JD. The continuum of dental caries – evidence for a dynamic disease process. *J Dent Res* 2004;83(Spec Iss C):C39–42.
- [39] Hefferren JJ, Koehler HM. Foods, nutrition and dental health. Park Forest South: Pathotox Publishers; 1981.
- [40] Chow LC, Takagi S, Shih S. Effect of a two-solution fluoride mouthrinse on remineralization of enamel lesions in vitro. *J Dent Res* 1992;71:443–7.
- [41] Langhorst SE, O'Donnell JNR, Skrtic D. In vitro remineralization of enamel by polymeric amorphous calcium phosphate composite: quantitative micro-radiographic study. *Dent Mater* 2009;25:884–91.
- [42] Staninec M, Nalla RK, Hilton JF, Ritchie RO, Watanabe LG, Nonomura G, et al. Dentine erosion simulation by cantilever beam fatigue and pH change. *J Dent Res* 2005;84(4):371–5.
- [43] Mishra P, Palamara JE, Tyas MJ, Burrow MF. Effect of static loading of dentin beams at various pH levels. *Calcif Tissue Int* 2006;79(6):416–21.
- [44] Mishra P, Palamara JE, Tyas MJ, Burrow MF. Effect of loading and pH on the subsurface demineralization of dentin beams. *Calcif Tissue Int* 2006;79(4):273–7.
- [45] Koester KJ, Ager 3rd JW, Ritchie RO. The effect of aging on crack-growth resistance and toughening mechanisms in human dentin. *Biomaterials* 2008;29(10):1318–28.
- [46] Ivancik J, Arola DD. The importance of microstructural variations on the fracture toughness of human dentin. *Biomaterials* 2013;34(4):864–74.
- [47] Peterson RE. Stress concentration factors. New York: John Wiley and Sons; 1974.
- [48] Anusavice KJ. Phillips science of dental materials. 11th ed. Philadelphia: Saunders; 1996.
- [49] Murrell S, Marshall TA, Moynihan PJ, Qian F, Wefel JS. Comparison of in vitro erosion potentials between beverages available in the United Kingdom and the United States. *J Dent* 2010;38(4):284–9.
- [50] Lussi A, Jaeggli T, Zero D. The role of diet in the aetiology of dental erosion. *Caries Res* 2004;38(Suppl. 1):34–44.
- [51] Marquis RE. Oxygen metabolism, oxidative stress and acid-base physiology of dental plaque biofilms. *J Ind Microbiol* 1995;15(3):198–207.
- [52] Arola D, Galles LA, Sarubin MF. A comparison of the mechanical behavior of posterior teeth with amalgam and composite MOD restorations. *J Dent* 2001;29(1):63–73.
- [53] Asmussen E, Peutzfeldt A. Class I and Class II restorations of resin composite: an FE analysis of the influence of modulus of elasticity on stresses generated by occlusal loading. *Dent Mater* 2008;24(5):600–5.
- [54] Tasaka A, Tahara Y, Sugiyama T, Sakurai K. Influence of chewing rate on salivary stress hormone levels. *Nihon Hotetsu Shika Gakkai Zasshi* 2008;52(4):482–7.
- [55] Kruzic JJ, Nalla RK, Kinney JH, Ritchie RO. Mechanistic aspects of in vitro fatigue-crack growth in dentin. *Biomaterials* 2005;26(10):1195–204.
- [56] Moreau JL, Sun L, Chow LC, Xu HH. Mechanical and acid neutralizing properties and bacteria inhibition of amorphous calcium phosphate dental nanocomposite. *J Biomed Mater Res B Appl Biomater* 2011;98(1):80–8.
- [57] Liu Y, Tjäderhane L, Breschi L, Mazzoni A, Li N, Mao J, et al. Limitations in bonding to dentin and experimental strategies to prevent bond degradation. *J Dent Res* 2011;90(8):953–68.
- [58] Cheng L, Zhang K, Melo MA, Weir MD, Zhou X, Xu HH. Anti-biofilm dentin primer with quaternary ammonium and silver nanoparticles. *J Dent Res* 2012;91(6):598–604.